Integration of Power-to-Hydrogen Models in Power Systems Adequacy Assessments

Aurélia Hernandez
Institute of Mechatronic, Electrical Energy, and Dynamic Systems, UCLouvain
Louvain-la-Neuve, Belgium
aurelia.hernandez@uclouvain.be

François Vallée
Power Systems and Market Research Group, UMons
Mons, Belgium
francois.vallee@umons.ac.be

Emmanuel De Jaeger
Institute of Mechatronic, Electrical Energy, and Dynamic Systems, UCLouvain
Louvain-la-Neuve, Belgium
emmanuel.dejaeger@uclouvain.be

***Abstract*—In the context of the energy transition, green hydrogen is currently under the spotlight as it is perceived as a promising energy carrier to decarbonize the mobility and industry sectors. As the share of renewable energies in power system increases, so do the uncertainties. As a result, probabilistic adequacy studies have become crucial. This work aims to study the impact of hydrogen mobility demand on power systems adequacy assessment. To do so, an original model of the Power-to-Hydrogen conversion chain specifically tailored for Monte Carlo-based adequacy computations is proposed. The results allow to quantify to which extent an additional electrical demand from hydrogen electrolysis will impact the adequacy of a system.**

***Index Terms*—Adequacy assessment, Hydrogen, Linear interpolation models, Power-to-Hydrogen, Water electrolysis.**

I. Introduction

The European Union (EU) has set ambitious targets for the coming years in terms of greenhouse gas (GHG) emissions reduction: a 40% cut from the 1990 levels by 2030 and carbon neutrality by 2050. In this context, the energy sector has a significant role to play and must undertake an energy transition. Green hydrogen, defined as hydrogen produced through water electrolysis with electricity produced using renewable energy, is perceived as a promising energy carrier that could help decarbonize the mobility and the industry sectors. Indeed, hydrogen is a potential fuel for heavy transportation and a feedstock for industries. The transport and industry sectors are responsible for respectively 25% and 15% of EU's GHG emissions [1] and are hard-to-decarbonate sectors because part of their applications cannot be electrified. Therefore, studying the integration of green hydrogen in energy systems is relevant. As part of this energy transition, significant grid uncertainties appear due to intermittent renewable energy sources (RES), and probabilistic adequacy studies have become crucial to assess the reliability of the electrical grid.

In the literature, the integration of Power-to-Gas and Power-to-Hydrogen in energy systems has been studied from several points of view. The economic feasibility and opportunities of the technology were studied in [2], [3] and [4]. The characteristics (nominal vs. part load operation, capacity ranges, flexibility, investment and maintenance costs) of different types of electrolyzers are analyzed and compared in [5]. The impact that electrolyzers could have on the economic dispatch of power systems (operation costs, wind curtailment, congestion) is examined in [6]. The placement and the sizing of the Power-to-Gas facilities in the grid are optimized in [7]. Integrated electricity and gas system models are developed in [8] and [9], and in [10], the reliability of such systems is assessed. However, to the best of the authors' knowledge, no studies have yet been done on the impact that a certain hydrogen demand can have on the electrical grid from an adequacy perspective. That is, how does an additional electrical load from hydrogen production impact the adequacy of the electricity system.

Hence, the present work aims to study the impact that a hydrogen demand related to the mobility sector can have on the adequacy of power systems. To do so, two Power-to-Hydrogen (P2H) models (non-linear and linear) describing the steady-state behavior of an electrolyzer are developed and integrated into a sequential Monte Carlo adequacy computation tool.

The first P2H model which describes the relation between the hydrogen production and the electrical power consumption is non-linear. As non-linear models require higher computation time, a second P2H model which is a linear interpolation approximating the real response of the non-linear model is elaborated to speed up the Monte Carlo evaluation. Both models are integrated into the sequential Monte Carlo adequacy computation tool and tested on the Belgian Power System. The effective performance of the linear approximation is assessed through a comparison of the adequacy results' accuracy. Then, several scenarios will be tested with different annual quantities of hydrogen demand and different hourly profiles. This allows to assess the impact of P2H on the adequacy of power systems.

The work presented in this paper is structured according to the following sections: Section II outlines the generic P2H model and its linearized counterpart is developed in Section III. Section IV develops the hydrogen mobility profiles that are integrated into the case study. Section V resumes the sequential Monte Carlo process used to assess the adequacy. Section VI describes the case study which is representative of the Belgian Power System. Section VII compares both models and analyses the results of the different scenarios. Section VIII concludes the work of this paper.

II. Power-to-Hydrogen Model

The P2H conversion chain is composed of a rectifier, a buck converter and an electrolyzer stack. The rectifier transforms

the AC voltage from the grid into a DC voltage, and the buck converter is used to control the voltage given to the electrolyzers terminal to adapt the production of hydrogen. Indeed, electrolyzers need to be fed by a DC-voltage source, and the current flowing through them determines the quantity of hydrogen produced. In this work, the power electronics are considered ideal and have an efficiency of 1, i.e the P2H conversion chain model represents mainly the electrolyzer stack.

A. Electrolyzer technologies

Electrolyzers use elecricity to split the water molecule H_20 into hydrogen and oxygen. For the time being, only Alkaline and Polymer Electrolyte Membrane (PEM) electrolyzers are commercially available. Though the Alkaline technology is the most mature, PEM electrolyzers are the most promising for future applications and still can be improved in terms of current density, dynamics and efficiency unlike the Alkaline technology that has reached its maximum performances [11]. For these reasons, PEM electrolyzers are considered in this study.

B. Voltage of electrolysis cell

The energy required to initiate the electrolysis, $\Delta H = \Delta G + T\Delta S$ does not have to be entirely supplied by electrical energy. Since entropy ΔS increases in this process of dissociation, part of the energy of reaction can be brought from the environment at a certain temperature T. The amount of energy that has to be brought under the form of electricity is the Gibbs free energy ΔG. The electrical contribution is supplied to the PEM cell under the form of an electrical potential, also called the reversible voltage :

$$V_{ocv} = \frac{\Delta G}{zF} \tag{1}$$

where $z = 2$ is the number of electrons transferred during the reaction and F the Faraday's constant.
However, in practice, the electrical potential is higher than the reversible voltage because of thermodynamic irreversibilities. Indeed, when current flows through the cell, losses of different nature appear.

- *Ohmic losses* represent the resistance of the electrodes and cell components to the electron flux and the resistance of the membrane to the ion flux [11].
- *Mass transport losses* represent the limited supply of reactant water to the process and the reduction of catalyst utilisation due to diffusion and bubbles phenomena respectively [11].
- *Activation losses* represent the electrochemical kinetics of the half reactions at the cathode and anode, i.e. the energy required to transfer the electrical charge between chemical species and electrodes [11].

C. Equivalent electrical circuit (EEC) of large-scale PEM electrolyzer

When dealing with large-scale electrolyzers, some assumptions can be made regarding the losses. In Ayivor's work [12], the following assumptions are made relying on [11]:

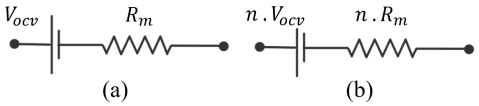

Fig. 1: Simplified Equivalent Electrical Circuit (EEC) of (a) large-scale electrolyzer cell and (b) large-scale electrolyzer stack.

- Mass transfer losses are not significant for low and moderate current densities and can be neglected up to 3 A/cm²,
- Activation losses are especially dominant at low current densities,
- Ohmic losses becomes dominant at mid current densities.

The resulting simplified electrical equivalent circuit (EEC) of a large-scale PEM cell in steady-state conditions is illustrated in Fig. 1a.

An electrolyzer stack is formed by the connection in series of n electrolysis cells. Thus the EEC of a PEM stack can be modelled by an equivalent reversible voltage $n * V_{ocv}$ and a total membrane resistance of $n * R_m$ (see Fig. 1b). The mathematical relation between the electrical power injected in the stack and the hydrogen production is developed hereunder.

1) Stack current: The hydrogen production rate of a cell $m_{H_2,cell}$ is proportional to the current thanks to the derivative with respect to time of the Faraday equation (2). Since the cells are in series, the stack production rate m_{H_2} is n times the cell production rate as shown in (3) and the current I can thus be expressed in function of the stack production rate.

$$m_{H_2,cell} = \frac{I}{F}\frac{M}{z} \quad \text{[g/s]} \tag{2}$$

$$m_{H_2} = n\frac{I}{F}\frac{M}{z} \quad \text{[g/s]} \leftrightarrow I = m_{H_2}\frac{zF}{nM} \quad \text{[A]} \tag{3}$$

where M= 2.016 [g/mol] is the molar mass of H_2.

2) Stack power: The mathematical expression of the stack power depends on the EEC that is used to model the electrolyzer stack. In this work, the relation between the stack current and the electrical power (Fig. 1) is quadratic and can be defined as:

$$\begin{aligned} P_{stack} &= V_{stack}I = (nR_mI + nV_{ocv})I \\ &= nR_mI^2 + nV_{ocv}I \end{aligned} \tag{4}$$

3) Stack power and H_2 production: With (3) and (4), the relation between the H_2 production and the stack power is derived in (5).

$$P_{stack} = nR_m(m_{H_2}\frac{zF}{nM})^2 + nV_{ocv}(m_{H_2}\frac{zF}{nM}) \tag{5}$$

D. Characteristics of the PEM electrolyzer

The characteristics of the PEM electrolyzer used in this study come from Ayivor's work [13] and are referenced in Table I. Thanks to these data, the relation between electrical power and hydrogen production of the EEC model expressed in (5) is represented in Fig. 2 (black line). This electrolyzer

unit can produce up to 20.65 [kg/h] at its nominal power of 1 MW.

TABLE I: Characteristics of the PEM electrolyzer stack from [13].

P_{nom}	J_{nom}	V_{ocv}	P_{min}	R_m
1 MW	3 A/cm^2	145 V	0.26 MW	0.015 Ω

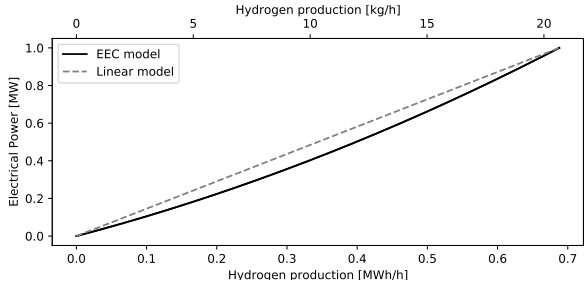

Fig. 2: Relation between electrical power and hydrogen production of the electrolyzer stack.

The EEC model is quadratic but rather close to linear. It could thus be interesting to establish a linearization of the mathematical relation and compare both models in the context of adequacy studies. This could indeed improve time computation of the electrical demand related to hydrogen mobility in the Monte Carlo process.

III. Linear Interpolation Model

The mathematical relation of the quadratic EEC model is linearized with the following constraints to guarantee physical consistency:

- No hydrogen is produced when no power is consumed which constrains the linear function to be affine.
- The hydrogen production at the nominal power of 1 MW is maximum and has a value of 20.65 kg/h.

This amounts to an interpolation of the quadratic EEC model through the points (0,0) and $(m_{H_2,max}, P_{nom})$. The linearized relation for a large-scale PEM electrolyzer can be expresed as:

$$P_{stack} = \frac{P_{nom}}{m_{H_2,max}}\ m_{H_2} \quad [MW] \tag{6}$$

Thus, the linear interpolation model of the electrolyzer used in this study is expressed as:

$$\begin{aligned} P_{stack} &= \frac{P_{nom}}{m_{H_2,nom}}\ m_{H_2} = \frac{1[MW]}{20.65[kg/h]}\ m_{H_2} \\ &= 48.48[MWh/ton]\ m_{H_2} \end{aligned} \tag{7}$$

and is represented in Fig. 2 (dashed gray line).

One of the many advantages of a linear model, is that electrolyzers can be aggregated together and considered as an equivalent electrolyzer. Indeed, the relation stays linear, unlike with the quadratic EEC model, electrolyzers have to be considered individually and cannot be aggregated together because the relation becomes discrete.

IV. Hydrogen Mobility Profile

In this work, the integration of hydrogen mobility demand is implemented. In order to distribute an annual hydrogen demand E_{H_2} among the 8760 hours of the year, different hourly profiles will be tested and compared. Firstly the hourly hydrogen demand will be fixed following a classical, uniform and wind-correlated profile. Secondly, the annual hydrogen demand will be distributed in an optimal way.

A. Fixed Profiles

1) Classical profile: The annual demand E_{H_2} is divided equally through the days of the year, then an hourly factor distribution f_h representing the classical distribution of transport departures during the day (represented by the black line in Fig. 3) is applied:
$$E_{H_2,h} = f_h * \frac{E_{H_2}}{365} \quad [MWh] \tag{8}$$
2) Uniform Profile: E_{H_2} is uniformly distributed through the 8760 hours of the year (see gray line in Fig. 3):
$$E_{H_2,h} = \frac{1}{24} * \frac{E_{H_2}}{365} \quad [MWh] \tag{9}$$
3) Wind-correlated Profile: The hourly distribution is different for each day of the year and is correlated to the hourly offshore wind power load factor lf_h:
$$E_{H_2,h} = \frac{lf_h}{\sum_{h=1}^{8760} lf_h} * E_{H_2} \quad [MWh] \tag{10}$$

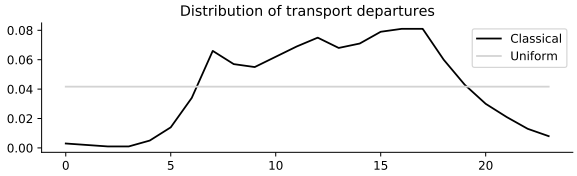

Fig. 3: Hourly distribution of transport departures during the day [-].

B. Flexible Profile

The annual hydrogen demand is distributed in an optimal way among the hours of the year. The total hourly production of the 8760 hours of the year will have to equal the annual hydrogen demand.

V. Adequacy study

Sequential Monte Carlo simulations are used to assess the adequacy of the power system and the process is depicted in Fig. 4.

A. Conventional Generating Units

The availability of the conventional generating units is represented using a two-state model. For each Monte Carlo year, the yearly availability profile of each unit is determined by a random sample draw from the time-to-failure TTF and

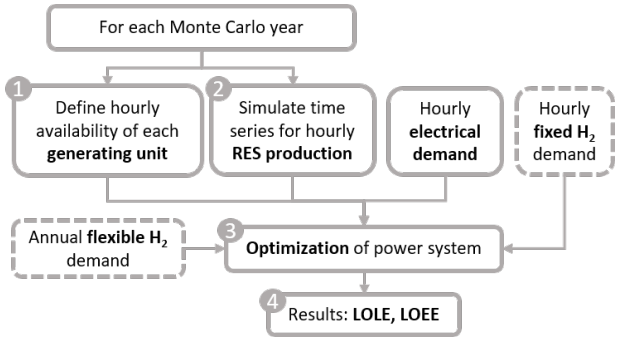

Fig. 4: Adequacy calculation scheme.

time-to-repair TTR distributions. TTF and TTR have negative exponential distributions and are defined as follows:

$$TTF_{sample} = -MTTF * ln(1-u) \quad [hours] \tag{11}$$

$$TTR_{sample} = -MTTR * ln(1-u) \quad [hours] \tag{12}$$

where u is a random sample from the uniform distribution, and $MTTF$ and $MTTR$ represent the mean TTF and mean TTR of each generating unit.

B. Wind Power

For each Monte Carlo year, an hourly profile is generated thanks to an auto-regressive and moving average (ARMA) model which is built based on historical data.

C. Optimization of Power System

$$\text{Min} \sum_{t=1}^{8760} \sum_{g=1}^{n_g} c(g) * P(g,t) + voll * Ens(t) \tag{13}$$

subject to :

$$P(g,t) \leq \alpha(g,t) * p_{max}(g) \tag{14}$$

$$\sum_{g=1}^{n_g} P(g,t) + res(t) + Ens(t) + P_{hs,out}(t) - P_{hs,in}(t) = l(t) + C(t) + \left(\frac{1}{\eta_{el}} + c_c\right) * (Q_{H_2,flex}(t) + q_{H_2,fix}(t)) \tag{15}$$

$$\sum_{t=1}^{8760} Q_{H_2,flex}(t) + q_{H_2,fix}(t) = q_{H_2,dem} \tag{16}$$

$$Soc_{phs}(t) = Soc_{phs}(t-1) + \eta_p P_{hs,in}(t) - \frac{P_{hs,out}(t)}{\eta_t} \quad \forall t > 1 \tag{17}$$

$$Soc_{phs}(t) \leq soc_{phs,max} \quad \forall t \tag{18}$$

with $P(g,t)$ the hourly production [MWh/h] of generator g, $Ens(t)$ the hourly energy-not-served [MWh/h], $P_{hs,out}(t)$ and $P_{hs,in}(t)$ the hourly energy [MWh/h] output and input of the pumped hydro storage (PHS), $C(t)$ the hourly curtailed energy [MWh/h], $Q_{H_2,flex}(t)$ the hourly flexible hydrogen production [MWh/h], and $Soc_{phs}(t)$ the hourly state-of-charge [MWh] of the PHS, being the variables of the formulation and n_g the number of generators, $c(g)$ the cost [€/MWh] of generator g, $voll$ the value of loss load [€/MWh], $\alpha(g,t) \in$ [0,1] the hourly availability of generator g, $p_{max}(g)$ the maximum capacity [MW] of generator g, $res(t)$ the hourly renewable power [MWh/h], $l(t)$ the hourly load [MWh/h], η_{el} the electrolyzer efficiency, c_c the compression efficiency, $q_{H_2,fix}(t)$ the hourly fixed hydrogen production [MWh/h], $q_{H_2,dem}$ the annual hydrogen demand [MWh/y], η_p and η_t the efficiencies of the PHS pump and turbine respectively, and $soc_{phs,max}$ the maximum capacity [MWh] of the PHS, being the parameters of the formulation.

D. Sequential Monte Carlo Simulation

This optimization formulation is ran for every Monte Carlo year. The loss-of-load LOL_y [hours/year] and loss-of-energy LOE_y [MWh/year] expressed in (19) and (20) are calculated for each Monte Carlo year and the adequacy indicators LOL-expectation (LOLE) and LOE-expectation (LOEE) expressed in (19) and (20) are derived for each simulation.

$$LOL_y = \sum_{t=1}^{8760} c_t \longrightarrow LOLE = \frac{\sum_{y=1}^{n} LOL_y}{8760} \tag{19}$$

$$LOE_y = \sum_{t=1}^{8760} Ens(t) \longrightarrow LOEE = \frac{\sum_{y=1}^{n} LOE_y}{8760} \tag{20}$$

In (19) and (20), c_t is a boolean variable that equals 1 if load is curtailed at hour h and 0 if not, and n is the number of Monte Carlo years in a simulation which depends on the convergence indicator

$$\epsilon = \frac{\sigma(X)}{\sqrt{n}E(X)} \tag{21}$$

where X represents the LOLE and LOEE respectively.

VI. Belgian Power System: Base Case study

The power system studied in this work is representative of the Belgian Power System considered as a 1 node system to which a hydrogen demand is added.

A. Conventional Generating Units

There are 86 conventional generating units in the system ranging from 5 to 425 MW with a total capacity of 6596.3 MW.

B. Wind Power

The offshore wind power capacity of Belgium is supposed to be 4.4 GW (forecast value for 2028). The hourly load factor for each Monte Carlo year is generated with the following ARMA model and whose order are set with the F-criterion method:

$$y_t = 0.236y_{t-1} + 1.482y_{t-2} + 0.167y_{t-3} + 0.563y_{t-4} + \epsilon_t + 0.71\epsilon_{t-1} - 0.86\epsilon_{t-2} - 0.645\epsilon_{t-3}. \tag{22}$$

The historical data used to build this model are the hourly load factors of the aggregated offshore wind power in Belgium [14] during the years 2017-2020.

C. Electrical Load

The hourly mean electrical load of the years 2018-2019 seen by the Belgian Transmission Grid Operator (Elia) is used as the deterministic load profile.

D. Annual Hydrogen Demand

The annual distance travelled by gasoline and diesel cars in Belgium during 2017 was n_{km} = 85 465 [10^6.km] [15]. Scenarios where part of the diesel and gasoline cars are replaced by fuel cell electric cars (FCEV) will be simulated, with a replacement share r_{sh} ranging from 0 to 20%. The annual hydrogen demand can thus be expressed as:

$$q_{H_2} = r_{sh} * n_{km}/100 * c_{H_2} \quad [kt/y] \tag{23}$$

with c_{H_2} = 1 [kg/100km] the consumption of a FCEV [16]. The annual hydrogen mobility demand with different replacement share are given in Table II.

TABLE II: Hydrogen replacement share [%] corresponding to the hydrogen quantity [kt/y].

%	**2**	**4**	**6**	**8**	**10**	**12**	**14**	**16**	**18**	**20**
$[kt/y]$	17.1	34.2	51.3	68.4	85.5	102.6	119.7	136.7	153.8	170.9

VII. Results

Firstly, the EEC model and the linear interpolation model are compared. Secondly, the impact of a hydrogen mobility demand on the Belgian Power System is analyzed.

A. EEC model vs. Linear Interpolation Model

1) Accuracy of adequacy results: The EEC model and the linear interpolation model are both integrated into the sequential Monte Carlo process and their results in terms of LOLE and LOEE are compared in Table III.

TABLE III: LOLE and LOEE comparison between EEC model and linear interpolation model with classical transport distribution.

	LOLE [h]			**LOEE [GWh]**		
H2 car share [%]	EEC model	Linear model	Error [%]	EEC model	Linear model	Error [%]
20	7.37	7.41	0.53	3.21	3.33	3.5

The error between both models is quite small and stays below the 0.53% and 3.5% for the LOLE and LOEE indicator respectively. This clearly demonstrates that the EEC model can be linearized when integrated to adequacy studies without impacting the accuracy of adequacy indicators.

2) Computation time : To produce the hydrogen necessary for a replacement share of 10% of the diesel and gasoline mobility fleet by fuel cell vehicles, about 900 electrolyzers of 1MW are necessary. The computational time to calculate the corresponding electrical load of this hydrogen mobility demand is 23 times longer with the non-linear EEC model than with the linear interpolation model (see Table IV).

TABLE IV: Computational time of EEC model and linear interpolation model to calculate the corresponding electrical load of a yearly hydrogen mobility demand (8760 hours) with a replacement share of 10% ($\sim$ 900 electrolyzers units of 1MW).

	EEC model	**Linear int. model**
Computational time	16 ms	0.7 ms

B. Sensitivity Analysis of the Hourly Distribution of the Hydrogen Mobility Demand

The Belgian Power System presented in Section VI with different hourly distribution of the hydrogen mobility demand is optimized within a sequential Monte Carlo process and the comparison in terms of LOLE and LOEE are represented in Fig. 5.

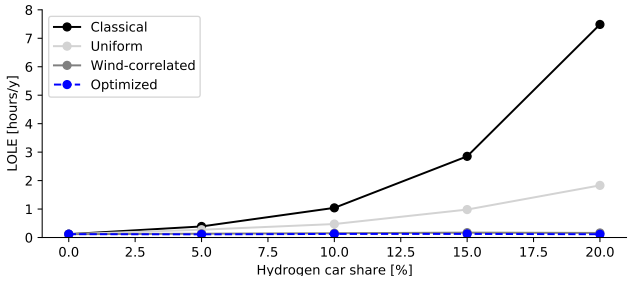

(a) LOLE indicator [hours/y]

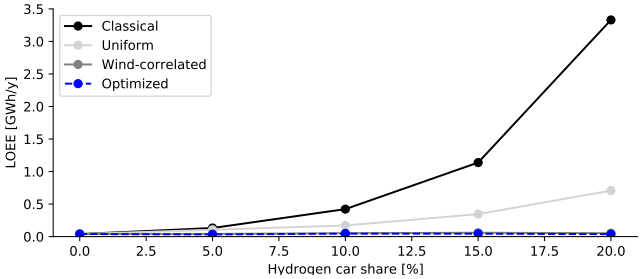

(b) LOEE indicator [GWh/y]

Fig. 5: Adequacy indicators of the different scenarios with progressive hydrogen car share up to 20%.

All scenarios except the optimized one show an exponential increase of the indicators, but with different exponents. For each replacement share, Table V gives the increase factor of the LOLE and LOEE indicators compared to the situation where no hydrogen mobility is added to the system, that is:

$$\text{LOLE Increase factor} = \frac{LOLE_{sh}}{LOLE_{sh=0\%}} \tag{24}$$

$$\text{LOEE Increase factor} = \frac{LOEE_{sh}}{LOEE_{sh=0\%}} \tag{25}$$

where $LOLE_{sh}$ is the LOLE of the scenario with a specific H_2 car share sh and $LOLE_{sh=0\%}$ the LOLE of the Belgian Power System without any hydrogen mobility demand.

TABLE V: The increase factor of the LOLE and LOEE indicators of scenarios with different hydrogen car shares.

	H_2 **car share**	**5%**	**10 %**	**15 %**	**20 %**
LOLE	Classical	3.3	8.83	24.17	63.46
	Uniform	2.32	4.01	8.32	15.52
	Wind-correlated	1.13	1.28	1.4	1.4
	Optimized	1	1	1	1
LOEE	Classical	3.35	10.7	28.86	84.45
	Uniform	2.67	4.34	8.75	17.95
	Wind-correlated	1.05	1.32	1.41	1.41
	Optimized	1	1	1	1

A first observation is that when the annual hydrogen demand is optimized throughout the year (flexible H_2 demand), no impact is observed on the adequacy until 20% of hydrogen car share while for the other scenarios (fixed H_2 demand), the impact is more or less significant depending on the scenario.

Already at 5% of hydrogen car share, the hourly distribution of hydrogen throughout the year has an impact on the adequacy indicators. Indeed, the LOLE and LOEE of the classical scenario increase by a factor 3.3 and 3.35 respectively while the LOLE and LOEE of the uniform scenario increase by a factor 2.3 and 2.7 respectively. This difference gets more significant as the hydrogen car share increases. The wind-correlated scenario has a very low impact on the adequacy indicators and is very close to the optimized scenario. It can be deduced that both scenarios produce hydrogen at similar moments, i.e. when wind power is important.

At 10% of hydrogen car share, the LOLE of the classical scenario is impacted 7 times more than the wind-correlated scenario, and the uniform scenario, 3 times more than the wind-correlated scenario. At 20%, the LOLE of the classical and uniform scenarios are respectively 45 and 11 times more impacted than the wind-correlated scenario.

The results show clearly that the hourly profile of the hydrogen mobility demand has a significant impact on the adequacy of power systems and that optimising the hydrogen demand, or correlating it to wind power is relevant.

VIII. Conclusion

This paper presents the impact that a hydrogen mobility demand can have on power systems adequacy assessments. To do so, a Power-to-Hydrogen (P2H) model is integrated into a sequential Monte Carlo computational tool. In this work, two models i.e a non-linear equivalent electrical circuit and its linear interpolation counterpart have been tested and compared on a case study representative of the Belgian Power System.

As a first result, it has been observed that the linear interpolation approximation does not impact the accuracy of adequacy results (0.5 and 3.5% error for LOLE and LOEE respectively) and that it can reduce the time computation by $\sim$23 when considering about 900 electrolyzer units of 1 MW (arbitrary production subdivision used to satisfy a 10% H_2 car share). This is useful to reduce computation time, especially when the P2H model is integrated within the Monte Carlo process, that is when the H_2 mobility demand is considered as a flexible load and is calculated at each time step. A second important result is that the hourly profile of H_2 mobility demand has a significant impact on the adequacy indicators. Firstly, when optimizing the H_2 demand, no impact is observed on the adequacy. Secondly, with a 10% share of H_2 fuel cell cars in the vehicle fleet, the LOLE of the power system with classical and uniform hourly H_2 mobility distributions is impacted 7 and 3 times more than with an hourly H_2 mobility distribution profile correlated with the offshore wind power production. This clearly shows the relevance to optimize the H_2 mobility demand profile or correlate it to wind power to reduce the hydrogen demand impact on power systems adequacy.

IX. Acknowledgment

The work is supported via the Belgian Energy Transition Funds project 'BEST' organized by the FPS economy.

References

[1] Aggregated GHG emissions by sectors — European Environment Agency.

[2] M. Jentsch et al. Optimal Use of Power-to-Gas Energy Storage Systems in an 85% Renewable Energy Scenario. *Energy Procedia*, 46:254–261, January 2014.

[3] C. Baumann, , R. Schuster, and A. Moser. Economic potential of power-to-gas energy storages. *10th International Conference on the European Energy Market (EEM)*, pages 1–6, May 2013.

[4] A. Belderbos et al. Possible role of power-to-gas in future energy systems. *12th International Conference on the European Energy Market (EEM)*, pages 1–5, May 2015.

[5] A. Buttler et al. Current status of water electrolysis for energy storage, grid balancing and sector coupling via power-to-gas and power-to-liquids: A review. *Renewable and Sustainable Energy Reviews*, 82:2440–2454, February 2018.

[6] V. Heinisch et al. *Effects of power-to-gas on power systems: A case study of Denmark*. June 2015.

[7] I. Diaz de Cerio Mendaza et al. Optimal sizing and placement of power-to-gas systems in future active distribution networks. *IEEE Innovative Smart Grid Technologies - Asia (ISGT ASIA)*, pages 1–6, November 2015.

[8] Y. Li et al. Day-ahead schedule of a multi-energy system with power-to-gas technology. pages 1–5, July 2017.

[9] Y. Xue, Y. Gao, Y. Li, F. Wen, K. Wang, Y. Huang, and Y. Xue. Optimal Coordinated Operation of Electricity and Natural Gas Distribution Networks with Power-to-Gas Facilities. *IEEE Innovative Smart Grid Technologies - Asia (ISGT Asia)*, pages 294–299, May 2018.

[10] S. Wang, , Y. Ding, C. Ye, C. Wan, and Y. Mo. Reliability evaluation of integrated electricity–gas system utilizing network equivalent and integrated optimal power flow techniques. *Journal of Modern Power Systems and Clean Energy*, 7(6):1523–1535, November 2019.

[11] T. Smolinka, E. Ojong, and T. Lickert. Fundamentals of PEM Water Electrolysis: Principles and Applications. In *PEM Electrolysis for Hydrogen Production : Principles and Applications*, pages 11–33. October 2015.

[12] P. Ayivor, J. Rueda Torres, M. van der Meijden, R. van der Pluijm, and B. Stouwie. Modelling of Large Size Electrolyzer for Electrical Grid Stability Studies in Real Time Digital Simulation. *3rd International Hybrid Power Systems Workshop*, 2018.

[13] P. Ayivor. *Feasibility Of Demand Side Response From Electrolyzers To Support Power System Stability*. PhD thesis, 2018.

[14] Elia Belgian TSO. Donnees de production eolienne.

[15] SPF Mobilité et Transport. Kilomètres parcourus par les véhicules belges en 2017.

[16] WaterstofNet. National implementation plan hydrogen refuelling infrastructure belgium.